Journal of Applied Mechanics and Technical Physics, Vol. 39, No. 2, 1998

BREAKING OF GRAVITY WAVES IN THE MOTION OF A VERTICAL PLATE IN A TWO-LAYER LIQUID

V. I. Bukreev

UDC 532.59

Results of experimental studies of surface and internal waves generated by translational motion of a vertical plate covering the entire cross section of the channel are discussed. It is found that the waves do not break at the critical propagation speeds predicted by the linear theory or the first approximation of shallow water theory. Breaking begins only at higher propagation speeds, at which the stabilizing effect of wave dispersion ceases. Quantitative information is given that can be used to test mathematical models and numerical methods.

When waves break, the ordered motion becomes partially chaotic. In this respect, breaking of waves is similar to laminar–turbulent transition. At the same time, unlike the turbulence problem, the transition of smooth waves to breaking waves has received little attention. The author is aware of just one mathematical model [1] that describes this transition.

The present paper reports results of an experimental study of changes in the wave pattern for a two-layer liquid of finite depth when the wave-propagation speed passes through the four possible critical values. The conditions under which the waves break are specified, the role of stabilizing and destabilizing factors is discussed, and the changes in the propagation speed and height of the waves during breaking is analyzed. Similar data for a liquid of uniform density are given in [2–5].

1. For a homogeneous liquid at rest above an even horizontal bottom, theoretical analysis gives two characteristic values of the propagation speed c of plane gravity waves. The value $c_1 = \sqrt{gh}$ (g is the acceleration of gravity and h is the initial depth of the liquid) is predicted by the linear theory as the limiting propagation speed of small harmonic perturbations. In transition to a region in which $c > c_1$, the waves can break or retain smoothness. In the experiments of [2–5], the waves remained smooth and their instability manifested itself only in the fact that weak oblique waves, whose growth was suppressed by surface tension, arose against the background of the main plane wave. The value $c_2 = \sqrt{2gh}$ is predicted by the second approximation of shallow water theory as the limiting speed of propagation of cnoidal (in particular, solitary) waves [6]. The more accurate value $c_2 = 1.294\sqrt{gh}$ is obtained on the basis of the complete model for potential liquid flow [7, 8].

The ambiguity of the characteristic speed makes it necessary to specify the terminology, which has not been universally accepted even for c_1. The most universal name of c_1 — the critical speed — is used in hydraulics. Its other names reflect a certain feature of the response of the system and are more "narrow." It has been suggested [5] that c_1 be called the first critical speed of propagation of gravity waves on shallow water and c_2 the second.

The experiments of [4, 5] confirmed the second of the indicated theoretical values of c_2 and showed that this speed is critical not only for solitary waves but also for waves of a more general type. In the vicinity of this speed, wave dispersion, a strong stabilizing factor, ceases to prevent destructive tendencies even when the nonlinearity is weak. Stabilizing factors such as nonstationarity or surface tension also turn out to be less effective. In the experiments, waves with speeds $c > c_2$ invariably break.

Lavrent'ev Institute of Hydrodynamics, Siberian Division, Russian Academy of Sciences, Novosibirsk 630090. Translated from Prikladnaya Mekhanika i Tekhnicheskaya Fizika, Vol. 39, No. 5, pp. 11–18, September–October, 1998. Original article submitted October 22, 1996; revision submitted February 5, 1997.

0021-8944/98/3905-0659 $20.00

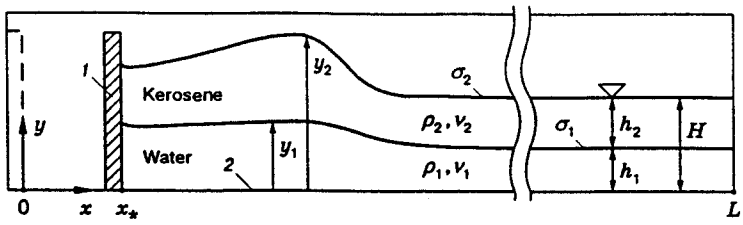

Fig. 1. Diagram of experiment: 1) plate; 2) bottom of the tank.

In the case of a two-layer liquid with a free surface there are two modes of natural vibrations: surface and internal. For each of them, at least two critical speeds exist. Theoretically, a pair of speeds similar in sense to c_1 is found from the dispersion relation of the linear theory of $c(k)$ for $k \to 0$ (k is the wavenumber of linear harmonic perturbations) [6]:

$$(c_{11}, c_{21}) = \sqrt{\frac{gH}{2}\left[1 \pm \sqrt{1 - \frac{4(1-\lambda)h_1 h_2}{H^2}}\right]}. \tag{1.1}$$

Here the first figure of the subscript indicates the free-boundary number and the second indicates the critical-speed number (the plus sign and the subscript 2 correspond to the surface wave), $H = h_1 + h_2$, $\lambda = \rho_2/\rho_1$, where h_1 and ρ_1 are the initial depth and density of the lower liquid and h_2 and ρ_2 are those for the upper liquid. The liquids do not mix with each other. The influence of viscosity and interface tension is not taken into account. From (1.1) it follows that the same value $c_1^* = \sqrt{gH}$ is obtained in all the three limits: $h_1 \to 0$, $h_2 \to 0$, and $\lambda \to 0$. The initial state with $\lambda > 1$ is unstable by the Rayleigh–Taylor mechanism. For $0 < \lambda < 1$, we have $c_{11} < c_{21} < c_1^*$.

Rigorous formulas for c_{12} and c_{22} are not available at present. Therefore, in planning experiments, one has to use approximate relations. The goal of the present work is to study the behavior of the waves in the vicinity of the highest critical speed c_{22}. To estimate this quantity, we used the following line of reasoning.

In practice, one has to deal with two droplet liquids for which λ is in the range of 0.8 to 1 or with a droplet liquid and a gas when $\lambda \ll 1$. In the second case, $c_{11} \to 0$ and $c_{21} \to \sqrt{gh_1}$, i.e., the influence of the difference in density on the first critical speed is insignificant and can be ignored. From the experiments of [4, 5] it follows that this conclusion is also valid for the second critical speed of the surface mode. The experiments were carried out for $\lambda = 0.8$. Analysis of (1.1) shows that the most significant effect of the difference in density takes place for $h_2/h_1 = 1$. In this case, $c_{11} = 0.224\sqrt{gH}$ and $c_{21} = 0.975\sqrt{gH}$, i.e., the effect of the difference in density is pronounced for the internal mode, whereas c_{21} differs from c_1^* by only 2.5%. As λ approaches 1, c_{21} differs little from c_1^*.

In view of the aforesaid, c_{22} was tentatively evaluated from the formula

$$c_{22} = 1.294\alpha\sqrt{gH}, \tag{1.2}$$

where

$$\alpha \approx \sqrt{\frac{1}{2}\left[1 + \sqrt{1 - \frac{4(1-\lambda)h_1 h_2}{H^2}}\right]}.$$

Formula (1.2) was also used to normalize experimental data.

2. A diagram of the experiment is shown in Fig. 1. A rectangular tank (3.8 × 0.2 m) with a horizontal bottom was filled with water ($\rho_1 = 1$ g/cm^3 and the kinematic viscosity $\nu_1 = 0.0101$ cm^2/sec) and kerosene ($\rho_2 = 0.8$ g/cm^3 and $\nu_2 = 0.0182$ cm^2/sec). In an analysis of the stability of surface waves and the energy losses due to breaking of them, it is necessary to take into account that in the experiments the third medium — air under normal laboratory conditions — was also present. The stability of the waves is strongly affected by interfacial tension on the boundary of contact between the different media. In particular, if interfacial

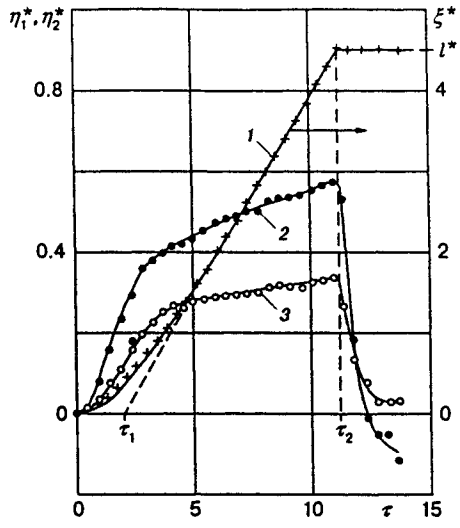

Fig. 2. Law of motion of the plate and variation of levels on it: law of motion (curve 1), free-surface level (curve 2), and interface level (curve 3).

tension is ignored, an arbitrarily small difference in speed on the contact boundary leads to development of the Kelvin–Helmholtz instability. In the experiments, the coefficients of interfacial tension between water and kerosene σ_1 and between kerosene and air σ_2 were 40 ± 6 and 27 ± 0.2 erg/cm^2, respectively. This ensured the Kelvin–Helmholtz stability up to a difference in speed of 15–20 cm/sec.

In the initial state, the liquid was at rest. At the moment $t = 0$, the vertical plate 1 began to move along the x axis, and at $t = T_2$, it suddenly stopped. The fixed coordinate system is shown in Fig. 1. The coordinate origin is on the line of intersection of the frontal plane of the plate with the bottom of the tank at $t = 0$. The plate covered the entire cross section of the tank. This particular case of submersion of the plate was studied to minimize the number of parameters of the introduced perturbation. The same purpose was pursued in the choice of the law of motion of the plate $x_*(t)$, where x_* is the coordinate of an arbitrary point on the plate.

Figure 2 (curve 1) gives an example of the law of motion of the plate obtained by filming. The following designations are adopted: $\xi^* = x_*/H$ and $\tau = t\sqrt{g/H}$. The experimental points are well approximated by the dependence

$$x_* = \begin{cases} Ut + UT_1[\exp(-t/T_1) - 1] & \text{for } 0 \leqslant t < T_2, \\ l & \text{for } t \geqslant T_2, \end{cases} \tag{2.1}$$

where U, T_1, T_2, and l are parameters, among which only any three are independent. Below, U, T_1, and T_2 are used as the main parameters. A two-parameter law of motion is realized in [4]. In experiments, a further reduction in the number of parameters is impossible.

The main quantities studied were the fluctuations of the interface y_1 and the free surface y_2 (see Fig. 1). Before the loss of stability, these quantities depended on x, t, and the parameters listed above. In the experiments U, T_1, T_2, and h_2/h_1 were varied. The remaining parameters, including $H = 4.8$ cm, were not varied. The quantities y_1 and y_2 were recorded by filming with a frequency of 32 frames per second. For the quantitative information presented below, the standard deviation of the error did not exceed 2% for the surface-wave speed and 3% for their height, and the corresponding characteristics for the internal waves were 3 and 4%, respectively.

3. Typical results of the experiments are given for the following combination of the main parameters: $H = 4.8$ cm, $h_2/h_1 = 1$, $\lambda = 0.8$, $U/\sqrt{gH} = 0.49$, $\tau_1 = T_1\sqrt{g/H} = 2.0$, and $\tau_2 = T_2\sqrt{g/H} = 11.1$ ($l^* = l/H = 4.42$). Figure 2 shows the law of motion of the wall precisely for this case. Graphs of the increase

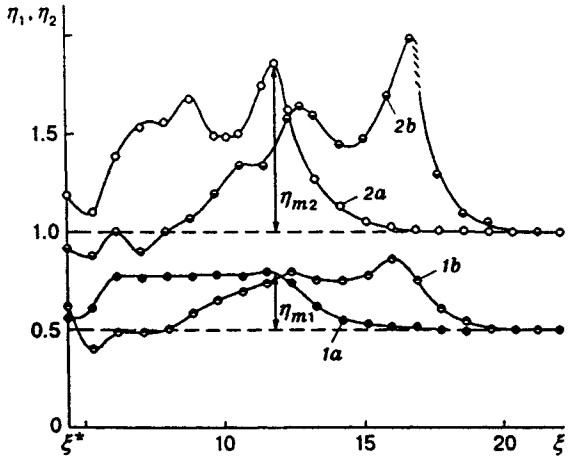

Fig. 3

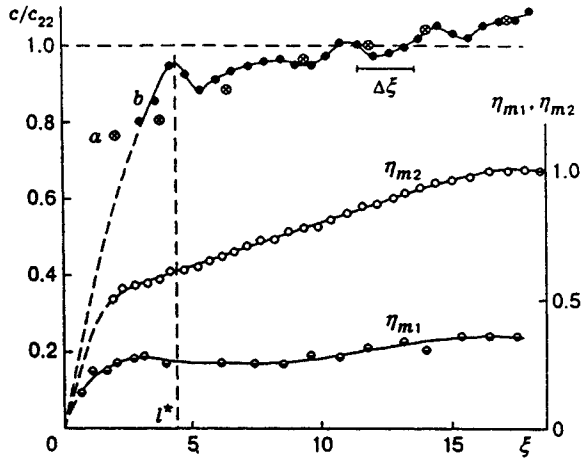

Fig. 4

Fig. 3. Wave profiles before and after breaking: curves 1a and 1b refer to η_{m1} and curve 2a and 2b refer to η_{m2}; $\tau = 12.0$ (curves 1a and 2a) and 15.6 (curves 1b and 2b).

Fig. 4. Propagation speeds and heights of waves: curves a and η_{m1} for the internal wave and curves b and η_{m2} for the surface wave.

in the levels of the free surface (curve 2) and the interface (curve 3) directly on the wall are also given in the figure. The following designations are adopted: $\eta_1^* = (y_1^* - y_{10})/H$ and $\eta_2^* = (y_2^* - y_{20})/H$, where y_1^* and y_2^* are the ordinates of the interface and the free surface at $x = x_*$ and y_{10} and y_{20} are the same quantities for the state of rest. Until the stop of the plate ($\tau < \tau_2$), η_1^* and η_2^* remained smooth. At $\tau > \tau_2$, their behavior became chaotic as a result of the drastic change of conditions on the plate due to its sudden stop. It is possible that at small distances downstream of the plate, loss of stability proceeds simultaneously by different mechanisms, including instabilities at lower critical speeds. Visually, here we observed the entrainment of air in kerosene and mixing of water and kerosene. At a certain distance from the stopped plate, the Kelvin–Helmholtz instability began to develop on the back slope of the internal wave. Nonstationarity and interfacial tension suppressed it, and the wave became smooth until the speed of propagation of its leading edge reached c_{22}. Then, breaking of the surface wave began, and the internal wave remained smooth until complete degeneration.

Figure 3 shows profiles of the surface wave and the internal wave at two times after the stop of the plate ($\eta_1 = y_1/H$, $\eta_2 = y_2/H$, and $\xi = x/H$). The speed of propagation of the leading edge of the perturbation (curves 1a and 2a) had just reached c_{22} from below, and the perturbation speed entered the supercritical region (curves 1b and 2b). In the interval $\xi^* < \xi < 6$, entrainment of air in kerosene and mixing of water and kerosene occurred. In the intervals $6 < \xi < 8$ and $6 < \xi < 12$, the Kelvin–Helmholtz instability was manifested for both waves (curves 1a and 1b, respectively).

Weak oblique waves were observed behind the leading edge, on the free surface, and on the interface. The occurrence of oblique waves is a manifestation of the loss of stability. It is possible that the presence of these waves is due to the fact that during evolution the perturbation intersected the boundary $c = c_{21}$. Nonstationarity, dispersion, interfacial tension, and viscosity prevented development of instability on this boundary to the breaking stage. However, it is possible that precisely oblique waves were those perturbations that led to breaking of the main wave in intersecting the boundary $c = c_{22}$.

Since the waves were nonstationary, it is necessary to specify the definition of their propagation speed c. Further, as c we use the speed of longitudinal motion of that point of the leading edge whose departure from the equilibrium position is equal to $\eta_m/2$, where η_m is the height of the first crest (Fig. 3). In this case, the speeds of propagation of other points of the leading edge differed from c by not more than 2%.

The dependence of c on ξ is given in Fig. 4. For $\xi > 7$, the difference in c between the surface wave

TABLE 1

h_2/h_1	c_{2E}/c_{22}	h_2/h_1	c_{2E}/c_{22}
0	1.00	1	0.99
0.1	1.10	2	0.97
0.2	0.99	5	1.01
0.5	0.97	11	1.02

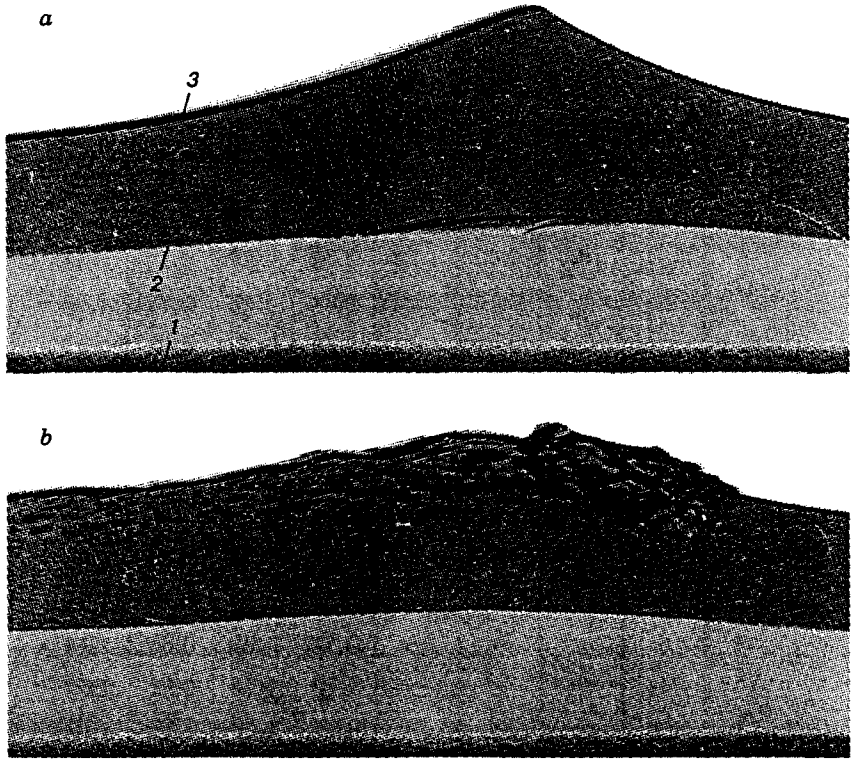

Fig. 5. Photographs of the head part of waves in the initial stage of breaking (a) and for fully developed breaking (b): 1) tank bottom; 2) interface; 3) free surface.

and the internal wave was within the limits of the measurement error. Filming showed that the transition of smooth to breaking surface waves proceeded on the interval $\Delta\xi$. Breaking began when c reached c_{22} from below. Entry to the region $c > c_{22}$ occurred only after the breaking had become fully developed.

When the parameters, in particular, the acceleration of the plate, were varied, the behavior of the system differed from the one discussed above. In particular, in the region $c > c_{22}$, the waves could also retain smoothness for some time. However, gradually, the speed of propagation of smooth waves reached a local maximum, then decreased to c_{22}, and finally breaking began. After completion of this process, the propagation speed could grow again.

Figure 4 shows data on the heights of the first wave crests η_{m1} and η_{m2}. Unlike the propagation speed, this wave parameter does not undergo characteristic changes in the critical state and continues to grow monotonically during transition of smooth to breaking waves. It reaches the largest value in the stage of fully developed breaking, and the value of the corresponding maximum strongly depends on the wave shape. For example, according to the theory of [7, 8], the limiting height of a solitary wave on a free surface is equal to 0.827 of the initial depth. For waves of a more general type in the experiments of [4, 5], their limiting heights

TABLE 2

	$\tau = 5.8$		$\tau = 11.3$		$\tau = 14.2$		$\tau = 15.8$	
	$\xi^* = 1.86$		$\xi^* = 4.42$					
ξ_0	η_1	η_2	η_1	η_2	η_1	η_2	η_1	η_2
0	0.78	1.48	0.84	1.59	0.52	0.90	0.46	1.02
1	0.76	1.44	0.84	1.57	0.55	0.95	0.44	1.00
1.9	**0.69**	**1.55**	—	—	—	—	—	—
2	0.69	1.55	0.81	1.57	0.59	1.05	0.50	0.96
3	0.61	1.27	0.76	1.60	0.68	1.25	0.50	0.98
4	0.55	1.08	0.76	1.46	0.70	1.42	0.60	1.14
5	0.52	1.04	0.77	1.57	0.73	1.45	0.67	1.29
5.8	—	—	**0.78**	**1.79**	—	—	—	—
6	0.50	1.00	0.79	1.65	0.74	1.65	0.68	1.38
7	0.50	1.00	0.60	1.23	0.72	1.47	0.74	1.44
8	—	—	0.56	1.08	0.73	1.43	0.78	1.64
9	—	—	0.52	1.04	0.78	1.70	0.75	1.47
9.6	—	—	—	—	**0.78**	**1.90**	—	—
10	—	—	0.50	1.02	0.79	1.61	0.76	1.44
11	—	—	0.50	1.00	0.60	1.21	0.81	1.61
11.9	—	—	—	—	—	—	**0.75**	**1.94**
12	—	—	0.50	1.00	0.57	1.06	0.74	1.69
13	—	—	—	—	0.53	1.03	0.60	1.23
14	—	—	—	—	0.51	1.00	0.56	1.11
15	—	—	—	—	0.50	1.00	0.52	1.09
16	—	—	—	—	0.50	1.00	0.51	1.03

were both greater and lower than the indicated theoretical limiting height of a solitary wave. In Fig. 4, the dimensionless limiting heights of the surface wave reaches unity, and at the beginning of the breaking process, it is $\eta_{m2} = 0.85$.

Figure 5 shows photographs of the wave heads in the initial stage of breaking and at the stage of fully developed breaking of the surface wave. The internal wave in Fig. 5b remains smooth, although its speed exceeds c_{22}. It retains smoothness up to complete attenuation of vibrations in the tank. This internal wave is generated by the surface wave and can be treated as an induced wave. In addition, it is not stationary. Therefore, the question of the existence of smooth stationary free waves with $c > c_{22}$ remains open. Nevertheless, the above example of a smooth internal wave with $c > c_{22}$ is interesting, because necessary conditions for retention smoothness are developed by the dynamic system itself rather than by a specially selected external action.

To analyze the influence of the parameter λ on surface waves, we performed additional experiments with homogeneous liquids: water and kerosene. Qualitatively, the wave pattern was identical, other conditions being equal. But the critical speeds c_2 were attained at smaller x for water than for kerosene (by about 10%). For a two-layer liquid, the critical situation occurred for intermediate values of x.

Table 1 illustrates the effect of the parameter h_2/h_1 on the ratio c_{2E}/c_{22}, where c_{2E} is measured experimentally and c_{22} is calculated by formula (1.2). On the whole, the difference between the experimental and calculated data is within the limits of the measurement error. An exception is the case of a very thin

upper layer (0.44 cm), where the experimental critical speed exceeds the calculated speed by 10%. Probably, this is due to the fact that for such a small distance between two free boundaries, the total effect of interfacial tension on each of them increased stability.

Table 2 lists data on the wave profiles $\eta_1(\xi_0)$ and $\eta_2(\xi_0)$ for four fixed values of τ. As before, time is reckoned from the beginning of motion of the plate, and the longitudinal coordinate is reckoned from its current position, so that $\xi_0 = \xi - \xi^*$. Values of ξ^* are given in the Table 2. The values of ξ_0 for which $\eta_2 = \eta_{m2}$ are bold. The values of the main parameters are the same as those in Fig. 3. At $\tau = 5.8$, the plate moved. The other data are obtained for free waves. At $\tau = 11.3$, the waves remained smooth. At $\tau = 14.2$, breaking of the leading edge of the surface wave occurred, and at $\tau = 15.8$, breaking of the surface wave was completely developed.

On the whole, the results of the experiments confirmed the hypothesis that for each mode of natural vibrations of the liquid, besides the well-known critical propagation speed at which wave breaking can occur, there is at least one even more critical speed. The quantitative value of the latter can be evaluated from the limiting speed of propagation of solitary waves. An example is given where one of the two free boundaries of a two-layer liquid retained smoothness in the supercritical region owing to nonstationarity, interfacial tension, and viscosity.

The author thanks A. V. Gusev for measurements and film processing.

This work was supported by the Russian Foundation for Fundamental Research (Grant No. 95-01-01164) and the Foundation of Integration Programs of the Siberian Division of the Russian Academy of Sciences (Grant No. 43).

REFERENCES

1. V. Yu. Lyapidevskii, "Equations of shallow water with dispersion. Hyperbolic model," *Prikl. Mekh. Tekh. Fiz.*, **39**, No. 2, 40–45 (1998).
2. K. Nadaoka, M. Hino, and J. Koyano, "Structure of the turbulent flow field under breaking waves in the surf zone," *J. Fluid Mech.*, **204**, 359–387 (1989).
3. M. Perlin, J. He, and L. P. Bernal, "An experimental study of deep water plunging breakers," *Phys. Fluids*, **8**, No. 9, 2365–2374 (1996).
4. V. I. Bukreev and N. P. Turanov, "Experiments with shallow-water waves generated by motion of the end wall of a tank," *Prikl. Mekh. Tekh. Fiz.*, **37**, No. 6, 44–50 (1996).
5. V. I. Bukreev, E. M. Romanov, and N. P. Turanov, "Breaking of gravity waves in the neighborhood of their second critical propagation speed," *Prikl. Mekh. Tekh. Fiz.*, **39**, No. 2, 51–567 (1998).
6. L. V. Ovsyannikov, N. I. Makarenko, V. I. Nalimov, et al., *Nonlinear Problems of the Theory of Surface and Internal Waves* [in Russian], Nauka, Novosibirsk (1985).
7. M. S. Longuet-Higgins, "On the mass, momentum, energy, and circulation of a solitary wave," *Proc. Roy. Soc. London*, **A337**, 1–13 (1974).
8. M. S. Longuet-Higgins and J. D. Fenton, "On the mass, momentum, energy, and circulation of a solitary wave. II," *Proc. Roy. Soc., London*, **A340**, 471–493 (1974).